Original Article

Bulletin of Pure and Applied Sciences.
Vol.37 D (Physics), No.2, 2018: P.146-157
Print version ISSN 0970 6569
Online version ISSN 2320 3218
DOI: 10.5958/2320-3218.2018.00020.9

Physical and Structural Studies of (30-x) BaO-xAl_2O_3-$69.5B_2O_3$-$0.5MnO_2$ Glasses

Mohamad Raheem Ahmed[1,*], M. Narasimha Chary[2], Md. Shareefuddin[2]

Author's Affiliations:
[1]Muffakham Jah College of Engineering and Technology, Osmania University, Hyderabad, Telangana 500034, India.
[2]Department of Physics, Osmania University, Hyderabad, Telangana 500007, India

Corresponding author:
Mohamad Raheem Ahmed
Assistant Professor,
Muffakham Jah College of Engineering and Technology,
Osmania University,
Hyderabad, Telangana 500034, India.

E-mail:
mdraheem@mjcollege.ac.in

Received on 26.06.2018,
Accepted on 12.11.2018

Abstract

(30-x) BaO-xAl_2O_3-$69.5B_2O_3$-$0.5MnO_2$ ($0 \leq x \leq 15$ mol%) (BABM) glasses have been prepared using melt quench method. In the present work, the main focus on the role of Al_2O_3 in the glass composition. Differential scanning calorimeter (DSC) studies show that a glass transition temperature (T_g) decreases with an increase of Al_2O_3 content which was explained on the basis of NBO's. The FTIR spectra exhibit to know BO_3 and BO_4 structural units, band assignments confirms Ba^{2+}, Mn-O and bending vibration of Al-O in [AlO_4]. The Raman band at~786 cm^{-1} has clearly shown the presence of aluminium bond. It has been found that an increasing the Al_2O_3 content increases the bond length of the Al-O bond in AlO_4 which leads to an increase in molar volume and decrease density.

Keywords: Barium alumino borate glasses, Physical properties, Structural studies.

1. Introduction

In recent years, the examination over the oxide glasses doped with transition metal ions (TM) has received widespread attention because of their attractive physical and chemical combinational properties. Several researchers are motivated towards transition metal ions doped glasses due to the fact regarding their interesting properties in accordance with spectroscopy and many other practical applications like fiber optical communication, fiber amplifiers, fiber lasers, memory devices, photo conducting properties, microelectronics, radiation sensitive materials and solid state laser [1,2]. In the class of all TM ions, manganese ion is especially fascinating as it exists in several valance states in several glass networks relies on the quantitative properties of modifier and glass formers, the size of ions , their field strength, mobility of the modifiers cation [3,4]. EPR is magnificent technique to capable of obtaining the information about the transition metal ions in oxide glasses and the ligand field changes around TM ions. In oxide glasses, dopant ions like manganese act as a probe for determination of glass structure and its application in solid state devices like zinc-carbon batteries, wide applications in ceramic industry [5,6]. In general, B_2O_3 is recognized as excellent glass former, with triangular borate units generally as boroxol groups. Primarily, borate glasses are prevalently

recognised for their good transparency, lower melting temperature, higher refractive index and dielectric constant values [7]. As per conditions of glass formation, some of the glass formers like Si^{4+} and B^{3+} ions (in B_2O_3 and SiO_2) have a rather high field strength that makes an absence of oxygen ion in the glass. In this way, low field strength alkaline earth oxides, which have generally introduced into the glass network [8]. When alkaline earth metal oxides add to the borate oxide, a part of the boron is modified to tetrahedral coordination to a particular limit after which nonbridging oxygens are formed [9]. A portion of the advantages in utilizing modifiers (alkali/alkaline) in borate glass details are to increase the thermal resistance and mechanical strength, enhanced aqueous capacity to concentrate TM ions, chemical durability and also reduced of melting temperature[10]. Barium oxide (BaO) act as a network modifier and break the network bonds, in the broken network strontium ions invade interstitial positions surrounded by non-bridging oxygens [11]. Aluminium oxide enters in the glass network as tetrahedron (the network forming) and octahedral (modifying) is depending on the Al_2O_3/BaO ratio when Al_2O_3/BaO ≤ 1 only four coordinated ions formed in the form of AlO_4 and for Al_2O_3/BaO > 1 form of AlO_6 groups[12,13].In glass composition, TM ions react with aluminium oxide forming Al-O-M bonds instead of sitting together to form M-O-M bonds. Accordingly, there will be huge changes within the optical and electrical characteristics of the glass material [14]. The presence of optimal quantity of Al_2O_3 within the glass network enhances mechanical, chemical resistance [15].

In the present work, FTIR, Raman spectra and physical properties are studied. We observed changes in structural units of BABM glass. The point of this article is to consider the impact of the addition of Al_2O_3 on the glass network and know the site symmetry around Mn^{2+} ions.

2. Experimental

2.1. Glass preparation

Mn doped Barium alumino borate glasses have been synthesized through a melt quenching process with composition (30-x) BaO-xAl_2O_3-69.5B_2O_3-0.5MnO_2 (0 ≤ x≤ 15 mol %)(BABM Glasses) in an electrical silicon carbide heating element furnace at a temperature 1100˚C in the air atmosphere. The chemicals used were analar grade of H_3BO_3, BaO, Al_2O_3 and MnO_2. These were weighed according to molar ratio and weighted for 10 grams. This mixture of raw material was filled in platinum crucible and placed in an electrical-heated furnace, which took nearly 50-60min to melt and get complete homogeneous melt. At room temperature, the prepared melt was quenched through pouring it over a preheated (150˚C) steel plate. The glasses were then annealed at 300˚C for 3 hr to relieve residual internal stress. BABM glasses have been observed to be transparent, brown in colour and thickness varied in the range 0.5-1.5mm shown in Fig.1. Table.1 shows the fine glass composition with their glass code used in the present investigation.

Figure 1: Images of prepared glass samples of BABM

Table 1: Details of the glass composition and glass transition temperature (T_g) values

Glass code	Composition (mole %)				T_g (°C)
	BaO	Al_2O_3 (x)	B_2O_3	MnO	
BABM0	25	5	69.5	0.5	597
BABM1	22.5	7.5	69.5	0.5	589
BABM2	20	10	69.5	0.5	586
BABM3	17.5	12.5	69.5	0.5	578
BABM4	15	15	69.5	0.5	577

2.2. Characterization

Prepared glass samples are immersed in xylene to measure density utilizing Archimedes principle. Glass samples were analyzed by X-ray Diffractometer Philips Xpert pro model with scanning speed of $2^0(2\theta)$ per minute to identify the amorphous nature. DSC measurements were carried out on a NETZSCH DSC 404F3 spectrometer system in the temperature range of 200–650^{0}C with a heating rate of 10^{0}C/min. FT-IR spectra of present glasses are noticed in the region from 400-2000 cm^{-1} by Shimadzu 8400S spectrometer. The Raman Spectra was recorded on JOBINYVON HR800 (HORIBA) Raman Spectrometer with a solid state diode laser; in the range 220-2000cm^{-1}. All the experimental measurements were carried out at room temperature (RT).

3. Result and discussion

3.1. XRD studies

The XRD pattern of an Mn^{2+} ion doped strontium alumino borate (BABM) glass samples has been manifested in Fig 2. X-ray diffraction is a valuable procedure as a result of its potential to find crystals in glasses if the crystals are of dimensions larger than usually 100nm [16]. The XRD graph of an amorphous solid material is unique in relation to that of crystal and has it an existence of a broad hump over the region rather than the sharp peak. The obtained XRD pattern of all the BABM glass samples showed a broad hump around 20˚-30˚, which clearly indicates amorphous nature.

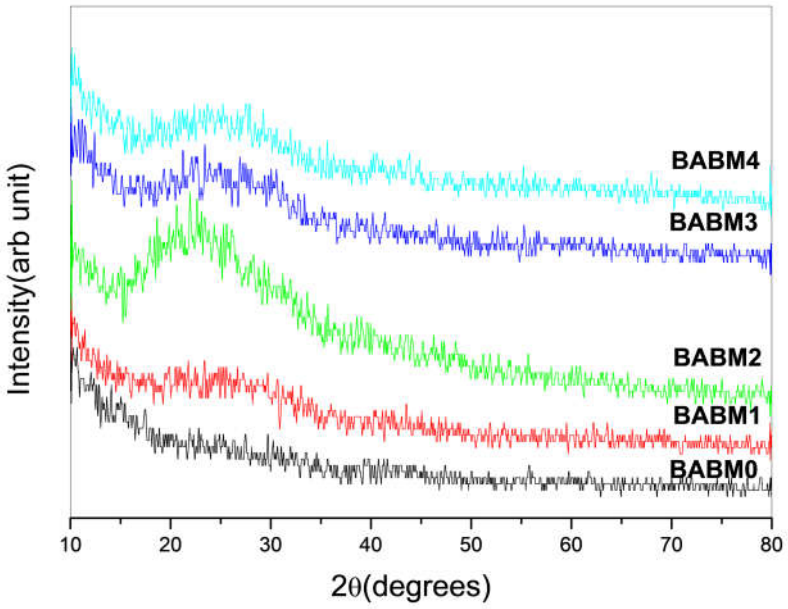

Figure 2: X-ray diffraction pattern for BABM glasses

3.2. Thermal analysis

DSC studies are mandatory for solids, especially for all types of organic and inorganic glasses since they provide glass transition temperature (T_g) and crystallization temperature (T_c). T_g is susceptible to variation of co-ordination number and formation of NBOs and strongly depend on the nature, strength of the chemical bonds. Increment of NBOs demonstrates the breaking of regular bonds which decrease the T_g. This behaviour is noticed an account of Al-O [ALO_4] bond count increases in the glass system which are much feeble than B-O bond [17,18]. Present glasses fall under this category and the corresponding DSC graph is shown in Fig.3 and its values are listed in Table.1. DSC for the present glass system are restricted to take upto 700˚c beyond this temperature samples are completely melted and damaged the boat. To know Tm and Tc, one sample is carried out upto 1200˚c is shown in

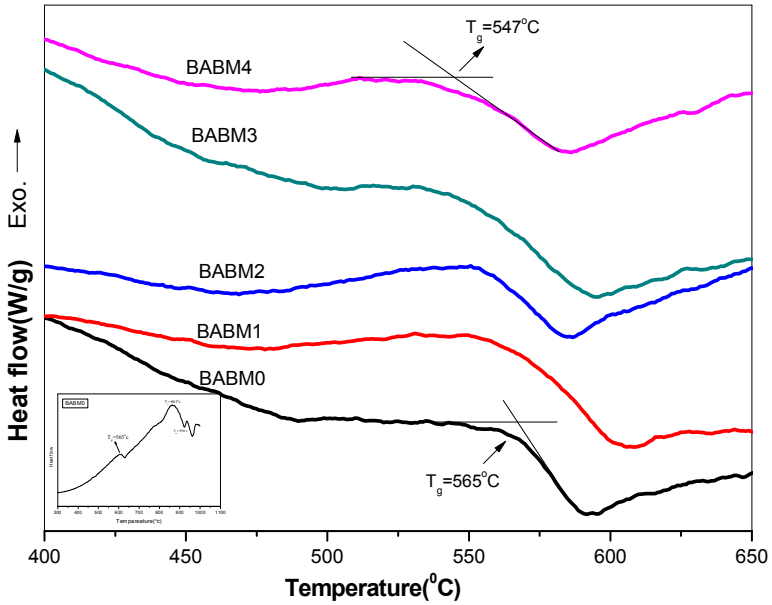

Figure 3: DSC curve of BABM glasses

3.3. Physical properties

Among various experimental techniques available to measure the density, the Archimedes principle is considered as the best choice to know structural changes in the glass. From the literature, it was observed that a slight change in the glass network causes abrupt changes in density values. A molar volume suggests an arrangement of building units and network modal of glasses. Boron and Aluminium familiar to possess over one stable configuration, i.e., boron exists as triangles of boron (BO_3) and tetraborate (BO_4), aluminium exists as a triangle of alumina (AlO_3) and tetrahedral alumina (AlO_4) [19,20]. Density values measured practically. These density values are employed to evaluate a corresponding molar volume of the glass samples. Both density (ρ) and molar volume (V_m) variation with Al_2O_3 content shown in Fig.4 and its values are given in the Table 2. It has been found that increasing the Al_2O_3 content increases the bond length of the Al-O bond in AlO_4, which successively is in direct proportionality to the V_m resulting in the creation of non-bridging oxygen (NBO). From the previous literature, it is understood that BaO acts as a modifier and convert BO_3 to BO_4 units which in general should decrease molar volume. But in the present case, BaO is being replaced by Al_2O_3 i.e., Al_2O_3 concentration increases from 5 to 15 mole percentage while BaO decreasing keeping other B_2O_3 and MnO content. Al_2O_3 consumes some of the oxygens form BaO readily converted to AlO_4. The remaining aluminium reacts with CuO suppress the process of converting BO_3 to BO_4

thereby resulting non-binding oxygens (NBO's) in the form of BO_3 units.The molar volume has a special association with the bond length and also plays an essential part in the experimental process. The bond length increases, which prompts an increase in molar volume is observed from different literature [19, 21].

$$\rho_{Ex} = \frac{Wt_a}{Wt_a - Wt_x} \times \rho_x \quad (1)$$

Where Wt_a is weight without liquid, i.e., in the air, weight in liquid, i.e., Wt_x in xylene respectively, and ρ_x is 0.863 g/cm^3.

$$V_M = \frac{M_W}{\rho_{Ex}} \quad (2)$$

Equation (2) is used to calculate the molar volume (V_M) and the corresponding terms in the above equation are mentioned in the reference [19]

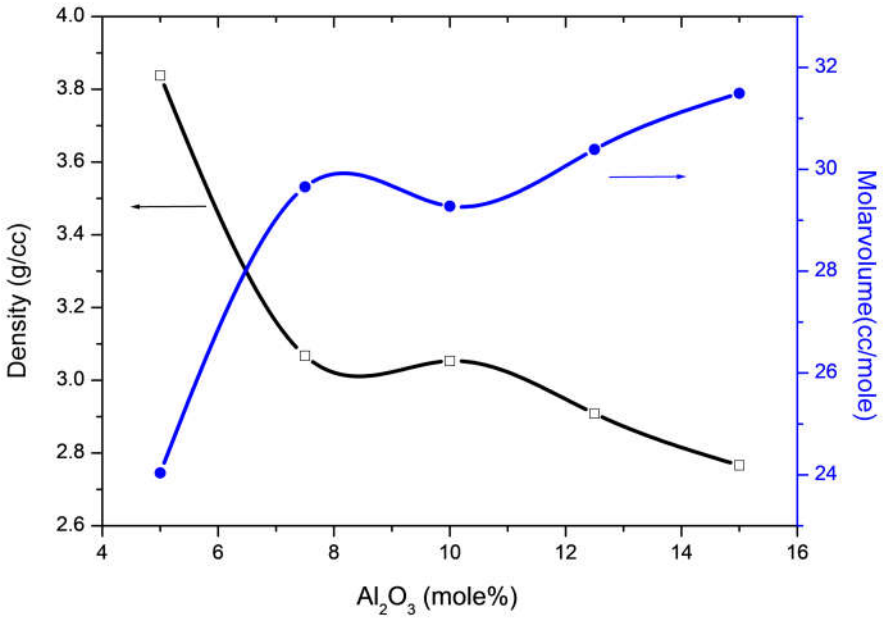

Figure 4: Density and Molar volume as a function of Al_2O_3 content of BABM glasses

To affirm the increase in molar volume the average boron-boron separation $< d_{B-B} >$ calculated [19] by using $V_m^B = \frac{V_m}{2(1-X_B)}$ in which V_m^B represents the volume that contains one mole of boron within the given structure while X_B is the molar fraction of boron trioxide $< d_{B-B} >= \left(\frac{V_m^B}{N_A}\right)^{\frac{1}{3}}$

where N_A is 6.0221×10^{23} being the Avogadro number. The values of boran-boran distance increases (0.478 to 0.522) progressively with an increment of Al_2O_3 (Table 2). The presence of Al_2O_3 helps to increase average boran-boran distance consequently leads to an increase in molar volume.

The refractive index (n_d) of BABC glasses has been related to the energy gap (E_g) through the relation is given by [6]

$$\frac{(n_d^2-1)}{(n_d^2+2)} = 1 - \sqrt{\frac{E_g}{20}} \quad (3)$$

where E_g is the energy band gap

The increment noticed in the values of refractive index (n_d) from 2.391 to 2.635 of the present system is as results of the raise in the NBO's count.

The refractive index (n_d) and dielectric constant (ε) are related as [6,19]

$$\varepsilon = n_d^2 \quad (4)$$

The values of ε and n_d are presented in Table 2. The molar refractivity R_M of the glass samples was evaluated using [6,19]

$$R_M = \left[\frac{{n_d}^2-1}{{n_d}^2+2}\right]{*}V_m \quad (5)$$

where n_d -refractive index, V_m - molar volume.
In search of understanding the parameters like polaron radius (r_p) and inter-ionic separation (r_i) the need arises for calculation of transition metal (TM) ion concentration per cc. In BAB glass system Mn^{2+} being TM ion, its concentration is calculated by the formula [17, 19]

$$N_i = \frac{N_A{*}X(mol\%){*}d}{M} \quad (6)$$

where $X(mol\%)$ refers to a transition metal ion, d- density, M - average molecular weight. The polaron radius (r_p) and inter-ionic separation (r_i) is calculated through the following relation [6,19]

$$r_p = \frac{1}{2}\left(\frac{\pi}{6N_i}\right)^{\frac{1}{3}} \quad (7)$$

and

$$r_i = \left(\frac{1}{N_i}\right)^{\frac{1}{3}} \quad (8)$$

The field strength is calculated using the oxidation number (Z) from the following formula [6,19]

$$F = \left(\frac{Z}{r_p^2}\right) \quad (9)$$

Table 2: Physical properties of BABM glasses

Physical property parameters		**x=5 mole%**	**x=7.5 mole%**	**x=10 mole%**	**x=12.5 mole%**	**x=15 mole%**
Glass code		**BABM0**	**BABM1**	**BABM2**	**BABM3**	**BABM4**
Average molecular weight M(g)		92.249	90.965	89.681	88.396	87.111
Density ρ(g/cm^3)(±0.001)	Experimental	3.837	3.067	3.053	2.908	2.766
	Theoretical	2.990	2.925	2.863	2.801	2.741
Molar volume (cm^3/mole)(±0.01)		24.037	29.656	29.861	30.390	31.492
Refractive index n_d		2.391	2.476	2.507	2.566	2.635
Molar Refractivity R_m(cm^{-3})		14.692	18.713	19.048	19.769	20.928
Dielectric constant ε		5.716	6.130	6.285	6.584	6.943
Reflection loss R%		0.1682	0.1803	0.1846	0.1928	0.2023
Transition metal ion		1.25	1.02	1.01	0.99	0.95

concentration (Ni) 10^{22}(ions/cc) (±0.01)					
Polaron radious(r_p) (A˚)(±0.005)	2.06	2.2	2.21	2.23	2.26
Inter-ionic distance (r_i) (A˚)(±0.005)	5.11	5.46	5.48	5.51	5.59
Molar polarizability α_m (A˚)^3	5.83	7.42	7.55	7.84	8.30
Field strength (F) (10^{15}cm^{-2})	4.71	4.13	4.09	4.02	3.92
Average boron-boron distance(d^{B-B}) (nm)	0.478	0.512	0.513	0.516	0.522
Optical band gap (E_g)(eV)(±0.01)	3.02	2.72	2.62	2.44	2.25
Urbach energy(eV)(±0.001)	0.167	0.368	0.260	0.385	0.507

In general polaron radius (r_p) and field strength should show the opposite trend which is clearly observed in the present work. The value of r_p increases from 2.06 to 2.26 A^0. This increment is attributed to the open structure caused by Mn^{2+} addition; the value of field strength (F) decreases also supports the open structure, which resulted in an increase in molar volume [17] as seen earlier. The polaron radius (r_p) and interionic distance (r_i) results are in tune with each other. The polaron radius in all the glasses (BABM series) is less than the corresponding interionic distance which in accordance with the usual prediction of the polaron theory that the polaron radius should be smaller than the site separation. [22]

3.4. FTIR studies

The FT-IR is an imperative tool for the examination of structure and dynamics of glass materials and providing information regarding functional groups. FT-IR spectra of SABM glasses in the span of 400 - 2000cm^{-1} are shown in Fig 5. The FT-IR band obtained for present glasses are centered at ~452, ~690, ~887, ~1032, ~1208, ~1375, ~1493, ~1594 cm^{-1}. The glass composition, band position and their assignment are summarized in the Table 3.

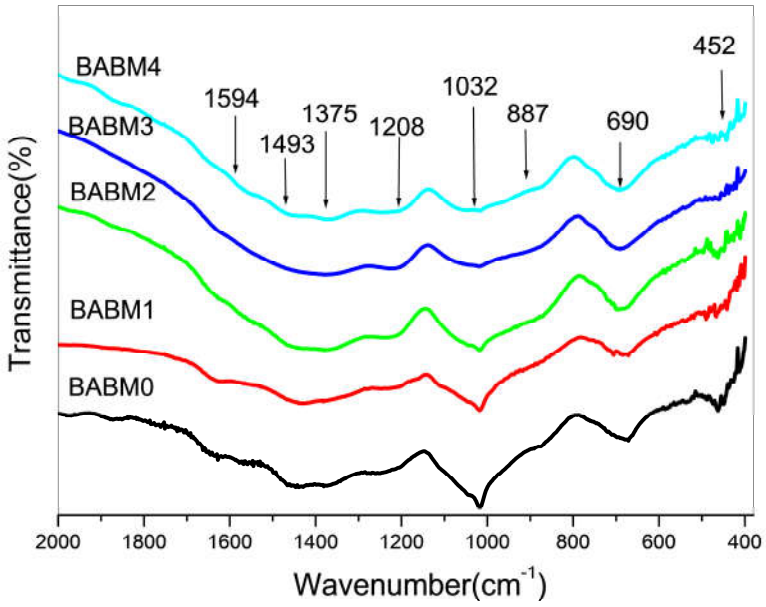

Figure 5: FT-IR spectra of BABM glasses

According to literature survey borate groups are mainly clarified into three regions:
(i) The first region 400- 887cm^{-1} which is assigned to the bending modes of different borate groups and the vibration of transition metal groups.

(ii) Second region 890- 1100cm^{-1} is due to the stretching of B-O in BO_4 due to the vibration of diborate to a penta borate group.
(iii) The third region fall in 1200- 1600cm^{-1} which label as stretching vibrations of borate units in BO_3 [23-30].

In the present work, the spectra exhibited a conventional band at 452cm^{-1} due to the vibration of metal cations (Ba^{2+}) and Mn-O(MnO_4) bond vibrations [23-26].The observed band around 690 cm^{-1} is allocated to the combined bending vibration of B-O-B in [BO_3] triangles and bending vibration of Al-O[AlO_4]. Consequently, an increase in the number of BO_3 units is expected causing an increase in the intensity of the bending band of these units and it is shifted towards longer wavenumber with increasing of Al_2O_3 mole percentage [26,27,28].The transmittance band ~ 887 cm^{-1} may be due to vibration of different borate groups [29,30]. By increasing Al_2O_3 content a considerable change in the position and intensity of ~690cm^{-1} peak was observed. The band is identified at 1032 cm^{-1} may due to the formation of B–O symmetric stretching vibrations of BO_4 units [27-31]. An additional band ~1208 cm^{-1} is due to B–O bond stretching vibrations and B–O bridging between B_3O_6 and BO_3 triangles [32, 33]. The band at 1375 cm^{-1} observed due to B–O stretching vibrations of trigonal BO_3 units[24-31]. Stretching vibrations of trigonal BO_3 groups are observed at 1493 cm^{-1} wave number [29].The presence of three bands around 1602 cm^{-1} is assigned to bending of O-H bonds and water molecules [24, 29, 31].

Table 3: FT-IR band assignment for BABM glass system

Glass code					Band assignment	References
BABM0	BABM1	BABM2	BABM3	BABM4		
460	452	454	455	452	Vibration of metal cations (Ba^{2+}) and Mn-O (MnO_4) bond vibrations.	[23-26]
682	685	685	685	690	Bending vibration of B-O-B in [BO_3] triangles and bending vibration of Al-O [AlO_4]	[26,27,28]
888	908	871	881	887	Vibrations due to tetrahedral tri-, tetra- and penta borate groups	[29,30]
1029	1028	1020	1020	1032	B–O symmetric stretching vibrations of BO_4 units	[27-31]
1214	1200	1214	1208	1208	B–O bond stretching vibrations and B–O bridging between B3O6 and BO3 triangles	[32, 33]
1369	1373	1373	1373	1375	B–O stretching vibrations of trigonal BO_3 units	[24-31]
1444	1522	1507	1527	1493	Stretching vibrations of trigonal BO_3 groups	[29]
1527	1602	1602	1602	1594	Bending of O-H	[24,29,31]

3.5. Raman studies
Recorded Raman spectra of present BABM glasses are exhibited in Fig. 6. The de-convoluted Raman spectra of BABM4 glass is shown in Fig 7. The BABM de-convoluted spectra have clearly revealed the Raman bands at ~286, ~326, ~484, ~527, ~647, ~757, ~918, ~1136,~1475, ~1650cm^{-1}.

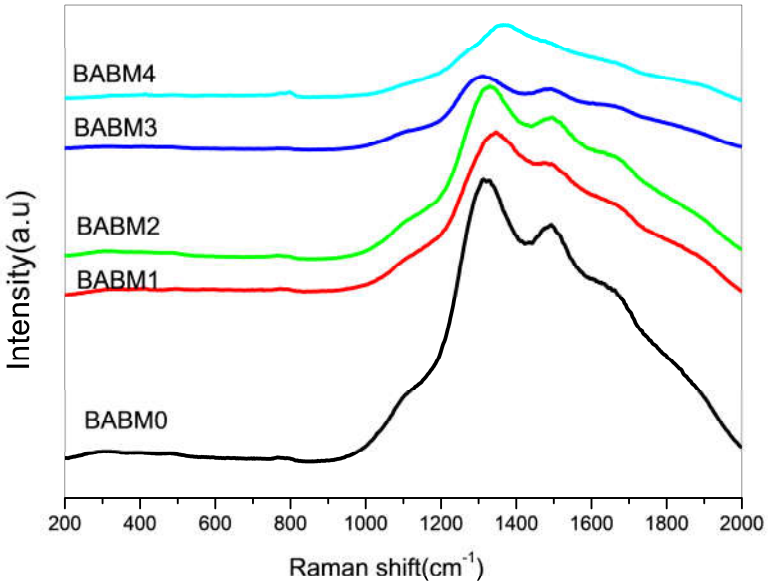

Figure 6: Raman spectra of BABM glasses

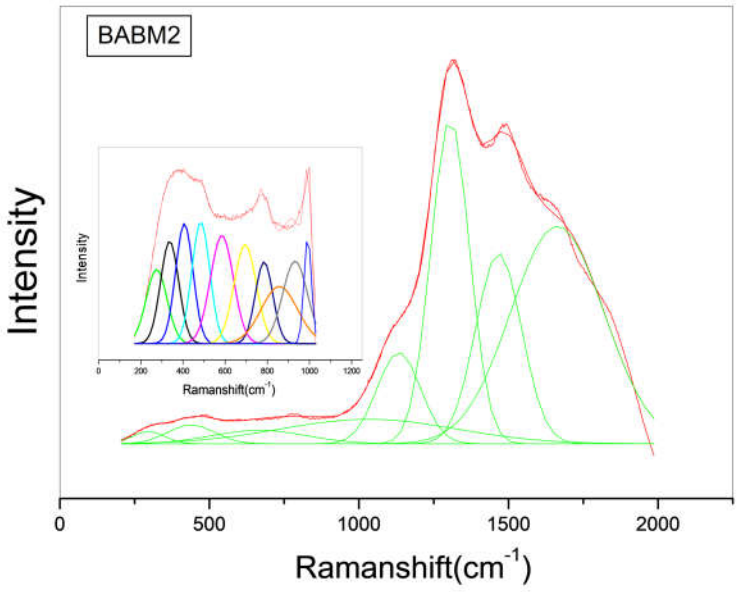

Figure 7: Deconvoluted graph of BABM4 glass

The BABM Raman band assignments are listed in Table 4. It is observed that the position, shape and intensities of the spectra changes with Al_2O_3 content. The band around 286 cm^{-1} is due to the metal cations observed in Raman spectra at lower Raman shift (<300cm^{-1}) [34]. The observed band near 326cm^{-1} is due to vibration of isolated tetrahedra. The band at ~484 cm^{-1} is assigned as existence of both B-O-B bend and Al-O-B bond. The band at ~527 cm^{-1} is observed as B-O-B stretching in BO_4 unit and corresponds to Al site(bridging Al-O-Al units). IR band nearly at 686 cm^{-1} is assigned as the symmetric vibration of metaborate rings. In the present composition, the fingerprints of the Al_2O_3 are clearly shown at peak nearly ~757 cm^{-1}. It is observed that the peak intensity is increasing with an

increment of Al_2O_3 content and shifting to higher Raman shift. An isolated six-membered ring of AlO_4 formed by corner-sharing of two oxygens per tetrahedron to give a structure with two non-bridged oxygens per AlO_4 tetrahedron. The Raman peak at ~918 cm^{-1} is observed due to assigned to the symmetric stretching of the B–O–B bridges and to the stretching of the terminal B–O bonds of the pyroborate groups. The centered band at ~1136 cm^{-1} is indicates the diborate units. The broad band at ~1475cm^{-1} is assigned as B–O Stretching vibration in BO_3 units in meta, pyroborate and orthoborate groups. The Raman band around 1650 cm^{-1} is due to $B–O^-$ vibrations of the BO_3 units attached to the large segment of borate network.

Table 4: Raman band assignments for BABM glass system

Glass code					Band Assignment	References
BABM0	BABM1	BABM2	BABM3	BABM4		
274	288	278	267	286	Metal cation bond vibration(Ba-O)	[32]
336	369	345	331	326	Vibration of BO_4 isolated tetrahedra	[33]
484	493	478	482	484	B-O-B bend and Al-O-B, aluminate network	[32, 33, 34]
584	576	565	557	527	B-O-B stretching in BO_4 unit and corresponds to Al site(bridging Al-O-Al units)	[37, 38, 39, 40]
695	680	693	643	647	Symmetric breathing vibration of metaborate rings	[35]
784	792	794	796	757	Ring breathing vibration of six membered rings contains both BO_3 triangles and BO_4 tetrahedral and stretching of AlO_4 units.	[41, 39, 40, 43]
897	892	896	912	918	assigned to the symmetric stretching of the B–O–B bridges and to the stretching of the terminal B–O bonds of the pyroborate groups	[42]
1135	1139	1133	1135	1136	Diborate group	[43]
1467	1480	1467	1451	1475	$B–O^-$ vibrations of the BO_3 units attached to the large segment of borate network	[44,45]
1612	1653	1663	1652	1650	Stretching vibrations of BO_3 triangles	[46,44]

4. Conclusions

It is from encapsulation, the overall features of the XRD patterns revealed the amorphous natures of BABM glasses. The experimental and theoretical values of density was calculated and observed that values are decreasing with increment of Al_2O_3 content and molar volume is increasing trend. This is due to higher Al-O bond length compare to nearby B-O bond length in BO_3 or BO_4. Al_2O_3 enters in the glass matrix and absorb some of the oxygens from BaO, creats AlO_4 with more number of NBOs which in turn decrease the Tg is observed by DSC. The concentration of BO_4 decreases in the glass network, whereas the concentration of BO_3 increases, it is also observed from FTIR and Raman bands. FTIR and Raman data were given the information about structural changes in the glass with an increment of Al_2O_3.

References

1. Sumalatha. B, Omkaram. I , RajavardhanaRao. T, LingaRaju. Ch (2013). The structural, optical and magnetic parameter of manganese doped strontium zinc borate glasses, *Physica B*. 411:99–105.
2. Kiran. N, Kesavulu. C.R, SureshKumar. A, Rao. J.L (2011) Spectral studies on Mn^{2+} ions doped in sodium–lead boro phosphate glasses. *Physica B*. 406:3816–3820..
3. Shiv Prakash Singh,. Chakradhar. R. P. S, Raob. J. L, Basudeb Karmakar (2010). EPR, optical absorption and photoluminescence properties of MnO_2 doped $23B_2O_3$-5ZnO-$72Bi_2O_3$ glasses. *Physica B*. 405*:* 2157-2161.
4. Rupesh Kumar. A, Rao. T.G.V.M, Veeraiah. N.V, Rami Reddy (2013). Fluorescence spectroscopic studies of Mn^{2+} ion in SrO-Al_2O_3-B_2O_3-SiO_2 glass system, *Optic. Mater.* 35: 402-406.
5. SivaRamaiah. G, LakshmanaRao. J (2012). Electron Spin Resonance and optical absorption spectroscopic studies of manganese centers in aluminium lead borate glasses. Spectrochi. *Acta Part A: Molec. Biomol. Spectr.* 98: 105–109.
6. Raghavendra Rao. T, Venkata Reddy. Ch, Rama Krishna. Ch, Sathish. D.V, Sambasiva Rao. P (2011). Ravikumar. R.V.S.S.N, Spectroscopic investigations and physical properties of Mn^{2+} doped mixed alkali zinc borate glasses. *Materi. Resea. Bulle.* 46: 2222–2229.
7. Pravinraj. S, Vijayakumar. M, Marimuthu. K (2017). Enhanced luminescence behaviour of Eu3+ doped heavy metal oxide telluroborate glasses for Laser and LED application. *Physica B 509:84*–93.
8. Tao Sun, HanningXiao, YinCheng, HuabinLiu (2009). Effects of MO (M=Ba, Mg, Ca) on the crystallization of B_2O_3–Al_2O_3–SiO_2 glass-ceramics. *Ceram. Inter.* 35:1051-1055.
9. Bahammam. S, Abd El Al. S, M. Ezz-Eldin. F (2017). Synthesis and characterization of c-irradiated cadmium-borate glasses doped V_2O_5*, Resu. Phy.* **7**: 241–249.
10. Haydar Aboud , Saad Saber , Wagiran. H, Hussin. R (2017). Energy response and thermo luminescence properties of lithium potassium borate Glass co-doped with Cu and SnO_2 nanoparticles, *J.Radi. Resea. Appl. Scien* 10: 1-5.
11. Prasanta Kumar Ojha, Rath. S.K, Chongsar. T.K, Gokhale. N.M, Kulakarni. A.R (2011). Physical and thermal behaviour of Sr-La-Al-B-Si bases SOFC glass sealants as function of SrO content and B_2O_3/SiO_2 ratio in the matrix. *J. Power. Sour.* 196: 4594-4598.
12. Rami Reddy. M, Bangaru Raju. S, Veeraiah. N (2001). Acoustic investigations on PbO-Al_2O_3 - B_2O_3 glasses doped with certain rare earth ions, *Bull. Mater. Sci*, 24: 63-68.
13. Dowidar. H (1998). Density-structure correlations in Na_2O-Al_2O_3-SiO_2 glasses. *J. Non.Crys.* 240: 55-65.
14. RameshBabu. P, Vijay. R, SrinivasaRao. P, Suresh. P, Veeraiah. N, KrishnaRao. D (2013). Dielectric and Spectroscopic properties of CuO doped multi-component Li_2O-PbO-B_2O_3-SiO_2-Bi_2O_3-Al_2O_3 glass system. *J. Non-Crys.* 370: 21-30.
15. Vijaya Lakshmia. P, Sambasiva Rao. T, Neeraja. K, Krishna Reddy. D.V, Veeraiah. N, Rami Reddy. M (2017). Influence of Mn^{2+} sensitizers on orange-red emission of Pr3+ ions in BaO–Al_2O_3–B_2O_3–SiO_2 glass system. *J.Lumin.*190: 379–385.
16. Sreekanth Chakradhar. R.P, Ramesh. K.P, Rao. J.L, Ramakrishna. J (2005). The effect of mixed alkali on EPR and optical absorption spectra in mixed alkali borate $x$$Na_2O$–$(30 - x)$$K_2O$–$70B_2O_3$glasses doped with iron ions, *J.Non-Cryst.* 351: 1289-1299.
17. Farouk. M, Samir. A, Metawe. F, Elokr. M (2013)., Optical absorption and spectral studies of bismuth borate glasses containing Er^{3+} ions. J. Non-Cryst. Solids. 371: 14–21.
18. Kim. E.A, Choi. H.W, Yang. Y.S (2015). Effects of Al_2O_3 on (1-x) [SrO-SiO_2-B_2O_3]-x Al_2O_3 glass sealant for intermediate temperature solid oxide fuel cell, Ceram. Intern 41: 14621-14626.
19. Pawar P.P, Munishwar. S.R, Gedam. R.S (2016). Physical and optical properties of Dy^{3}þ/Pr^{3}þ Co-doped lithium borate glasses for W-LED, *J. Alloys .Compd.* 660: 347-355.
20. Doweidar. H, Y.M. Moustafa, Abd El-Maksoud. S, Silim. H (2001). Properties of Na2O–Al2O3–B2O3 glasses. *Mate. Scie. Eng.* 301: 207–212.
21. Saddeek. Yasser B, Essam R. Shaaban, El Sayed Moustafa, Hesham M. Moustafa (2008). Spectroscopic properties, electronic polarizability and optical basicity of Bi_2O_3–Li_2O–B_2O_3 glasses. *Physica B* 403: 2399–2407.
22. Kumar. G. A, Thomas. J. et al (2000). Physical and optical properties of phthalocyanine doped inorganic glasses, *J. Mate. Sci.* 35: 2539 – 2542.

23. Chandra Sekhar. K, Abdul Hameed, Ramadevudu. G, Narasimha Chary. M (2013). Structural and crystallization behaviour of (Ba,Sr)TiO_3 borosilicate glasses, *Phase Trans.* 86: 1000-1016.
24. Gautam. C. R, Avadhesh Kumar Yadav (2013). Synthesis and Optical Investigations on (Ba,Sr)TiO_3 Borosilicate Glasses Doped with La_2O_3. *Optic. Photon. Journal.* 3: 1-7.
25. Putra Hashim Syed, Hashim Syed, Haji Abdul Aziz Sidek (2013). The Effect of Remelting on the Physical Properties of Borotellurite Glass Doped with Manganese, *Int. J. Mol. Sci.* 14: 1022-1030.
26. Padmaja. G, Kistaiah. P (2009). Infrared and Raman Spectroscopic Studies on Alkali Borate Glasses: Evidence of Mixed Alkali Effect, *J. Phys. Chem. A* 113: 2397–2404.
27. Singh. G. P, Parvinder Kaur, Simranpreet Kaur, Singh. D.P (2011). Role of V_2O_5 in structural properties of V_2O_5-MnO_2-PbO-B_2O_3 glasses. *Mater. Phys. Mecha.* 12: 58-63.
28. Vishal Kumar, Pandey. O.P, Singh. K (2010). Structural and optical properties of barium borosilicate glasses, *Physica B* 405: 204–207.
29. A.M. Abdelghany, F.H. ElBatal, H.A. ElBatal, F.M. EzzElDin, Optical and FTIR structural studies of CoO-doped sodium borate, sodium silicate and sodium phosphate glasses and effects of gamma irradiation-a comparative study, *J. Mole. Stru.* 1074 (2014) 503–510.
30. Abdel-Hameed, Marzouk. M.A (2018). Employing one crystalline phase to gain different phosphor emissions for distinctive applications: Preparation, crystallization and luminescence of $SrAl_2B_2O_7$ with different additions via glass ceramic technique, *J. Lumi.* 195: 67–78.
31. Limkitjaroenporn. P, Kaewkhao. J, Limsuwan. P, Chewpraditkul. W (2011). Physical, optical, structural and gamma-ray shielding properties of lead sodium borate glasses. *J. Phys. Chem. Solids.* 72, 245–251.
32. Chandkiram Gautam, Avadhesh Kumar Yadav, and Arbind Kumar Singh (2012). Review on Infrared Spectroscopy of Borate Glasses with Effects of Different Additives, *ISRN Ceram.* 2012 ,17.
33. Ardelean I, Peteanu. M, Ciceo-lucacel. R, Bratu. I (2000). Structural investigation of CuO containing strontium-borate glasses by means of EPR and IR spectrometry, *J.Mate. Sci: Mate. Elect.* 11: 11-16.
34. Chandkiram Gautam, Avadhesh Kumar Yadav, Vijay Kumar Mishra, Kunwar Vikram (2012). Synthesis, IR and Raman Spectroscopic Studies of (Ba,Sr)TiO3 Borosilicate Glasses with Addition of La2O3, *Open J. Ino. Non-met. Mate.* 2: 47-54.
35. Petru Pascuta, Rares Lungu, Ioan Ardelean (2010). FTIR and Raman spectroscopic investigation of some strontium–borate glasses doped with iron ions, J Mater Sci: Mat. Ele. 21: 548–553.
36. Edukondalu. A, VasantSathe , Syed Rahman, SivaKumar. K (2014). Thermal, mechanical and Raman studies on mixed alkali borotungstate glasses, *Physica B* 438: 120-126.
37. Daniel R. Neuville, Laurent cormier, Dominique massiot 2004. Al environment in tectosilicate and peraluminous glasses: A 27Al MQ-MAS NMR Raman, and XANES investigation, *Geo. Et Cosm. Acta*, 68: 5071–5079.
38. Rawan El Hayek, Fr´ed´erique Ferey, Pierre Florian, Daniel R. Neuville (2017), Structure and properties of lime alumino-borate glasses, *Chem. Geo.* 46: 75-81.
39. Shuai Kang, Xue Wang, Wenbin Xu, Xin Wang, Dongbing He, Lili Hu (2017). Effect of B_2O_3 content on structure and spectroscopic properties of neodymium-doped calcium aluminate glasses, *Opt. Mate.* 66: 287-292.
40. Paul McMILLAN (1983). Raman spectroscopy of calcium alumino glasses and crystals, *J. Non. Cryst*. 55: 221-243.
41. Raluca Ciceo-Lucacel, Ioan Ardelean (2007). FT-IR and Raman study of silver lead borate-based glasses, *J.Non-Cryst*. 353: 2020–2024.
42. Cristiane N. Santos, Domingos De Sousa Meneses et al (2009). Structural, dielectric, and optical properties of yttrium calcium borate glasses, *Appl. Phy. Lett*. 94:151901.
43. Mohamed Raheem Ahmed, Chandra Sekhar. K (2018). Abdul Hameed, Narasimha Chary. M, Shareefuddin. Md, Role of aluminum on the physical and spectroscopic properties of chromium-doped strontium alumino borate glasses, *Int. J. Moden. Phy. B,* 32:1850095.
44. Arunkumar. S, Marimuthu. K (2013). Concentration effect of Sm^{3+} ions in B_2O_3–PbO–PbF_2–Bi_2O_3–ZnO glasses structural and luminescence investigations, *J. Allo. Comp.* 565: 104–114.
45. Kirti Nanda, Neelam Berwal, Kundu . R. S, Punia. R, Kishore. N (2015). Effect of doping of Nd3+ ions in BaO-TeO_2-B_2O_3 Glasses: A Vibrational and Optical Study, *J. Molec. Stru*. 1088: 147-154.